Journal of Engg. Research Vol. 11 No(3A) pp.100-111 DOI:10.36909/jer.18597

Numerical Investigation of Liquefaction Potential in Sabkha Soil Supporting Foundation Subjected to Vibration Loading

Naif Alsanabani* and Ahmed Alnuaim*

**Department. of Civil Engineering, Engineering College, King Saud University, P.O Box 800, Riyadh, 11421, Saudi Arabia*

Corresponding author E-mail: alnuaim@ksu.edu.sa

Submitted **:** 14-06-2022

Revised **:** 21-09-2022

Accepted **:** 22-09-2022

ABSTRACT

Liquefaction is a major concern in loose soils subjected to vibrations, which may severely damage buildings and infrastructure. In this study, the influence of vertical vibrational loading on the liquefaction potential of natural sabkha soil was numerically examined to understand the effects of different parameters on the liquefaction potential. The parameters considered in this study included the vertical displacement amplitude, frequency, modified mass ratio, subsoil conditions (natural and cement-stabilized sabkha soils with 5% and 10% cement content), and thickness ratio of the cement-stabilized sabkha soil. Liquefaction was observed for different foundation configurations. The pore water pressure ratio beneath the foundation increased with a decrease in foundation mass. The minimum foundation mass that prevents liquefaction in the sabkha soil depends on the ratio of the machine velocity to the shear wave velocity of the subsoil (sabkha). This study provides guidance and information on the risk of constructing a foundation subjected to continuous vibration (such as machine foundations) in saturated sabkha soil because of the low rigidity resulting from the generation of pore water pressure during dynamic loading.

Keywords: Sabkha; Pore Water Pressure; Liquefaction; Vibration.

INTRODUCTION

Liquefaction is a major problem in geotechnical engineering, particularly under seismic and dynamic loads. It causes different types of damage to slopes, infrastructure, retaining walls, and foundations (Kramer, 1996). Liquefaction is a condition in which the pore water pressure (PWP) in cohesionless soil increases to a level where the effective stress becomes zero and the soil loses its strength. Initial liquefaction corresponds to the condition when PWP equals the confining pressure σ_3. In most cases, a 20% double-amplitude strain is considered a failure. Cyclic mobility is a liquefaction phenomenon triggered by cyclic loading in soil deposits with static shear stresses lower than the soil strength. Experimental and numerical studies on the liquefaction behavior of different soil types supporting foundations subjected to dynamic loading have been reported (Amini and Qi, 2000; El Fiky et al., 2020; Ibrahim, 2014; Lee, 2007; Mokhtar et al., 2014; Rollins and Seed, 1990; Vaid and Thomas, 1995; Yoshimi, 1967; Zeghal and Elgamal, 1994). Their results showed that liquefaction depends on the resistance of sand to deformation, and that the applied shear stress can reduce the volume or collapse of the structure. Liquefaction also depends on the sand fabrics, including gradation, particle size and shape, relative density, confining pressure, and initial stress state. Irregular cyclic loading caused by earthquakes is the most common cause of dynamic liquefaction.

To understand the liquefaction potential of sabkha soil, it is important to understand its basics. Sabkha has poor-to-medium density. Therefore, It is considered a problematic soil with liquefaction potential (Ahmed and Al Shayea, 2017). Sabkha soil is widespread in coastal semi-arid regions such as the Eastern and Western regions of Saudi Arabia. Some regions where sabkha soil is found have witnessed rapid increases in development, urbanization, and industrial activities. Some factories in such regions have reciprocating and centrifugal machines that require adequate support systems owing to the high vibrations induced by the machines. Machine foundations should satisfy dynamic requirements, which depend on the dynamic properties of the subsoil and the dynamic loading characteristics. Sabkha soil does not instantaneously collapse and requires a sufficient volume of water to dissolve the cementing agents, making it unsuitable for infrastructural support (Al-Amoudi and Abduljauwad, 1994, 1995; Al-Shamrani, 2004; Al-Shamrani and Dhowian, 1996). Ahmed and Al Shayea (2017) studied the liquefaction potential of sabkha soil under seismic loading and stated that loose soil layers cannot be liquefied for peak horizontal accelerations of more than 0.035 g. However, liquefaction is anticipated at higher Peak Horizontal Acceleration values (0.055, 0.07, 0.08, and 0.10 g) for subsurface profiles/zones with corresponding thicknesses of 6, 4, 3, and 2 m for loose sandy sabkha soil layers.

However, the liquefaction behavior of sabkha soil under vibrational loading has not been reported. Thus, in this study, the liquefaction of sabkha soil-supporting foundations subjected to vertical vibrations was numerically investigated by examining the excess PWP of points underneath the foundations at different displacement amplitudes and operating frequencies. The sinusoidal displacement amplitude that was applied to the foundation varied from 0.004, 0.04, and 0.0.4 mm and the operation frequencies were 5, 20, and 80 Hz. The influence of the foundation mass subjected to vertical vibration on the liquefaction behavior of natural sabkha was examined by varying the modified mass ratio (based on Eq. 5) as 0.012, 0.053, 0.15, and 0.06.

NATURAL SABKHA SOIL PROPERTIES

Evaluate the properties of the sabkha soil used in the numerical modeling is important. To evaluate the properties of sabkha soil, samples were collected from Ras Al-Ghar in Eastern Saudi Arabia. The field density, water content, sieve analysis, hydrometer analysis, Atterberg limits, and specific gravity of the sabkha soil were investigated according to ASTM standards (ASTM D2216-10, 2010; ASTM D422, 2007; ASTM D4318-10, 2010; ASTM D6938–10, 2010; ASTM D854, 2010). Their results, along with the results of the mineralogy tests, can be found in (Alnuaim et al., 2021). The general soil properties are listed in Table 1.

Table 1 Properties and classification of the sabkha soil (Alsanabani, 2021).

Property	Value
Specific gravity, Gs	2.78
Passing through # 200 (%)	27.74
Effective size, D_{10} (mm)	0.02
***D_{30} (mm)**	0.09
****D_{60} (mm)**	0.21
Coefficient of uniform, C_u	11.39
Coefficient of curvature, C_c	2.20
USCS Soil type	SM
AASHTO soil type	A-3

*D_{30} is the size at which 30% is finer by weight.

**D_{60} is the size at which 60% is finer by weight.

FINITE ELEMENT METHOD (FEM) MODELING

The FEM procedures consist of pre-processing, processing, and post-processing stages. The preprocessing stage compromises adjusting the meshing issues (element size, time size, and boundary conditions) that depend on the characteristics of the dynamic loading (magnitude, frequency, and phase angle) and the selection of the appropriate constitutive model. In the processing stage, the selected type of analysis (static, consolidation, or dynamic) and drain or undrained conditions are considered. In the final stage, the postprocessing stage displays the output results in terms of kinematics (displacement, strain, and strain rate) and kinetics (normal and tangential of the total or effective stresses and pore water pressure). Further details on these stages are provided in the following sections. The governing equation used in the dynamic analysis has three components: inertial force ($m\ddot{u}$), damping force ($c\dot{u}$), and stiffness force (Ku), which can be represented by Eq. (1) as:

$$m\ddot{u} + c\dot{u} + Ku = F(t) \quad (1)$$

where $\ddot{u}$, $\dot{u}$, and u are the acceleration, velocity, and displacement vectors, respectively; m is the mass matrix; c is the damping matrix; K is the stiffness matrix; F(t) is the external dynamic load vector, which varies with time (t). Nikam et al. (2021) presented a detailed description of the FEM solutions. The stiffness matrix depends on the constitutive model of the foundation material and subsoil (sabkha), where the capture of the decreasing stiffness of the saturated sabkha owing to the increase in the pore water pressure throughout the dynamic loading (in the undrained condition) should be considered by selecting an appropriate constitutive model, such as the UBC3D-PLM.

The liquefaction potential of saturated sabkha soil was numerically investigated using PLAXIS 3D software. The system consisted of a subsoil (natural sabkha) and a circular foundation subjected to sinusoidal cyclic vertical displacement amplitudes at frequencies of 5, 20, and 80 Hz. Owing to rapid cyclic loading, the sabkha was analyzed under undrained conditions. The foundation diameter was kept constant at 5 m. To eliminate the boundary effects on the FEM results, the FEM domain was six times the dimensions of the structure, as recommended by Bhatia (Bhatia, 2008). The analysis performed in this study was a quasi-static system; thus, the horizontal dimensions of the domain were 10 times the foundation diameter, and viscous boundary conditions were employed to eliminate the influence of the reflected waves. The relaxation coefficients for normal and tangential boundary conditions were set as 1.0 and 0.25, respectively (standard values) (MUÑOZ, 2008; Srivastava and Kumar, 2022)

Three elements were used in the analysis: (1) 10-node tetrahedral elements to simulate sabkha and cement-stabilized sabkha soil, (2) 6-node triangle plate elements to simulate foundations, and (3) 6-node elements to simulate structure–soil interfaces. Notably, one-quarter of the system was considered to reduce the calculation time. The size of the elements affects the accuracy of FEM analysis and depends on the wavelength transmitted through the element. Large or coarse elements may infiltrate the transmitted wave: the size of elements should be $\frac{1}{5}$ to $\frac{1}{8}$ of the wavelength (λ) (Kramer, 1996), which can be calculated based on the velocity (v) (compressive or shear) and frequency (f) using ($\lambda = vf$). The shear wave velocities of the sabkha samples were measured using a bender element and were 85, 120, and 211 m/s for effective confining stresses of 50, 100, and 150 kPa, respectively (Alnuaim et al., 2020). Operating frequencies of 5, 20, and 80 Hz were considered in the FEM analysis; therefore, the lower bound of the element size was approximately 0.3 m.

For wave propagation, the time step should be considered small such that the wave does not travel more than the element length in each step; otherwise, the results will be unreliable. The time step depends on the wavelength of the highest velocity, that is the p-wave. According to (Bhatia, 2008) and (Bathe, 2006), the maximum time step size used is given as ($\Delta t_{increment} = \frac{L_{ele}}{v_s}$) where L_{ele} is the element length, and v_s is the shear wave velocity.

Constitutive model

The UBC3D-PLM was used to model the sabkha soil under cyclic loading to evaluate the liquefaction potential. The UBC3D-PLM model adopts elastic-plastic behavior with plastic hardening and can assess the increase in excess PWP under undrained conditions or the increase in densification under drained conditions under dynamic loading, as expressed in Eq. (1) (Petalas & Galavi, 2013) as

$$K^{p}_{G,secondary} = K^{P}_{G}\left(4 + \frac{n_{rev}}{2}\right) hard\ f_{dens} \quad (1)$$

where $K^{p}_{G,secondary}$, and K^{P}_{G} are the secondary and input plastic shear modulus factors, respectively; n_{rev} is the number of shear stress reversals from loading to unloading; f_{dens} is a multiplier factor (a user-input parameter to adjust the densification rule); and *hard* is a factor that corrects the densification factor for loose soil, which is expressed by Eq. (2) (Petalas & Galavi, 2013);

$$hard = min\left(1, max\ (0.5, 0.1N_{60})\right) \quad (2)$$

where N_{60} is the corrected SPT value.

Under undrained conditions, the excess PWP can be computed based on the bulk modulus of water (*Kw*), which varies with the step. K_w is calculated based on the soil porosity (n), undrained bulk modulus (K_u), and effective bulk modulus (K'), which depend on the plastic shear modulus (K^{p}_{G}) (Petalas & Galavi, 2013). Saturated sabkha soil was modeled using the UBC3D-PLM to consider the effect of excess PWP generated under vertical vibration loading. The parameters used in the UBC3D-PLM were categorized into stiffness, strength, and densification. Stiffness is stress dependent and increases with depth. The stiffness parameters for the UBC3D-PLM include K^{e}_{B}, $K^{e}_{G}, K^{p}_{G}, ne, me, and\ np$, which vary with depth. The strength parameters include φ_{cv}, φ_{p}, and c, and the densification parameters are *Rf*, f_{dens}, and f_{Post}.. The parameters are listed in Table 1.

FEM for sabkha soil

After selecting an appropriate constitutive model that captures the behavior of the soil under consideration, it is important to carefully evaluate the parameters used in the constitutive model to ensure accuracy. In this study, the strength parameters were set as the strength of natural sabkha soil (Alnuaim et al., 2020). The monotonic and cyclic behaviors of the soil at effective stresses of 50, 100, and 150 kPa were studied by Alnuaim et al. (Alnuaim et al., 2020). They evaluated the stiffness parameters of 18700, 20200, and 20300 kPa, which were employed as input data in this study. The K^{e}_{B}, K^{e}_{G} K^{e}_{G}, n_{p}, and R_{f} parameters were fine-tuned to enhance the FEA results compared to the experimental test in terms of stress-strain at different effective confining stresses (50, 100, and 150 kPa). Notably, m_e and n_e were initially set to 0.5. Fig. 1 shows the $q-\varepsilon_1$curves obtained from FEM analysis and experimental tests at effective stress (σ'_3) of 50 kPa, and they show good agreement. The densification parameters f_{dens} and f_{post} were adjusted to enhance the numerical results for the increase in excess PWP with the number of cycles compared to the experimental results. Fig. 2 compares the FEM and experimental results of excess PWP with *N* for an effective stress of 50 kPa. The UBC3D-PLM showed a high excess of PWP in the first cycle. The main limitation of the UBC3D-PLM model is that it cannot consider the anisotropic consolidation effect during primary loading, which results in higher excess PWP values during the first complete cycle (Petalas and Galavi, 2013).

The stiffness in the UBC3D-PLM model is stress-dependent and varies with depth. To accurately estimate the stiffness of natural sabkha soil at different stress levels, the soil was divided horizontally into three layers (layer-1, -2, and -3), and the thicknesses of the layers were computed. The effective stresses in the middle of layer-1, -2, and -3 were 50, 100, and 150 kPa, respectively. The UBC3D-PLM parameters for the three layers are listed in Table 1. The effective stress includes the weight of the soil and the stress induced by the structures. An approximation method was used to compute the stress induced on the soil structure (Budhu, 2015).

Table 1 UBC3D-PLM parameters of the natural sabkha soil

Items	Define item	Layer-1	Layer-2	Layer-3
K_B^e	Elastic bulk modulus	150	190.5	100
K_G^e	Elastic shear modulus	80	90	54
K_G^p	Plastic shear modulus	800	275	350
me	Elastic shear modulus index	0.5	0.5	0.5
ne	Elastic bulk modulus index	0.5	0.5	0.5
np	Plastic shear modulus index	0.3	0.5	0.8
φ_{cv}	Constant volume friction angle	33	33	33
φ_p	Peak friction angle	33	33	33
c	Cohesion	9	9	4
N_{60}	SPT value	5	5	5
f_{dens}	Densification factor	0.3	6	0.6
f_{post}	Post liquefaction factor	0.7	12	0.8
σ_t	Tension cut-off	0	0	0
R_f	Failure ratio	0.9	0.94	0.91
Start level (m)		0	-8.5	-11.5
End level (m)		-8.5	-11.5	-25
σ_3' at mid-layer (kPa)		50	100	>150

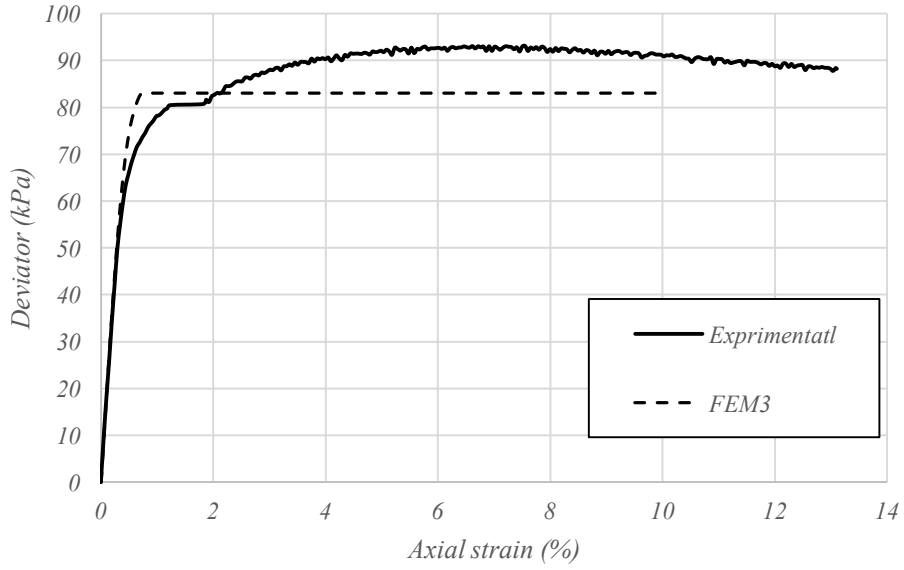

Fig. 1: Stress-strain for experimental and FEM for effective stress of 50 kPa

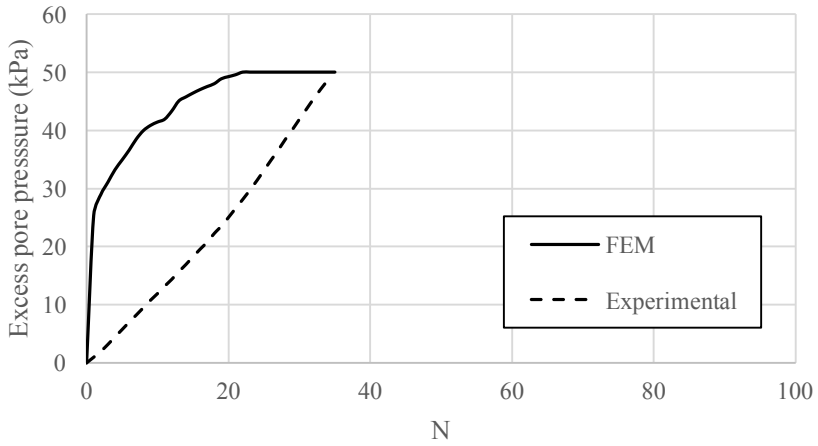

Fig 2: Excess PWP-N for experimental and FEM for effective stress of 50 kPa and *CSR* of 0.35

Parametric study

The effects of vertical displacement amplitude, frequency, and foundation mass on the liquefaction behavior of saturated salt-encrusted flat soil were investigated. In addition, the influence of the cement-stabilized sabkha layer underneath the vibrating foundation on the liquefaction potential was examined. The vertical displacement amplitudes were considered based on the maximum limit of the amplitude vibration in the machine performance and human tolerance. Based on the Baxter and Bernhart chart, which shows the permissible vibration for machine performance (Fig. 3 (a)), the boundary separated between “Slightly Rough” and “Rough regions” was marked (blue line), and the displacement amplitudes corresponding to operating frequencies of 5, 20, and 80 Hz were 0.5, 0.127, and 0.035 mm, respectively. Similarly, for human tolerance, the boundary edge between "Troublesome to person" and "Severe to person" regions was labeled (blue line) as shown in Fig 3 (b), and the displacement amplitudes corresponding to frequencies of 5, 20, and 80 Hz were 0.4, 0.04, and 0.004 mm, respectively. The lower bounds of the displacement amplitude were considered as 0.4, 0.04, and 0.004 mm.

The minimum frequency considered in the FEM analysis depends on the subsoil conditions and geometric foundation, as shown in Eq (3).

$$f_{min} = \frac{1}{2\pi r}\sqrt{\frac{G}{\rho}} \quad , \tag{3}$$

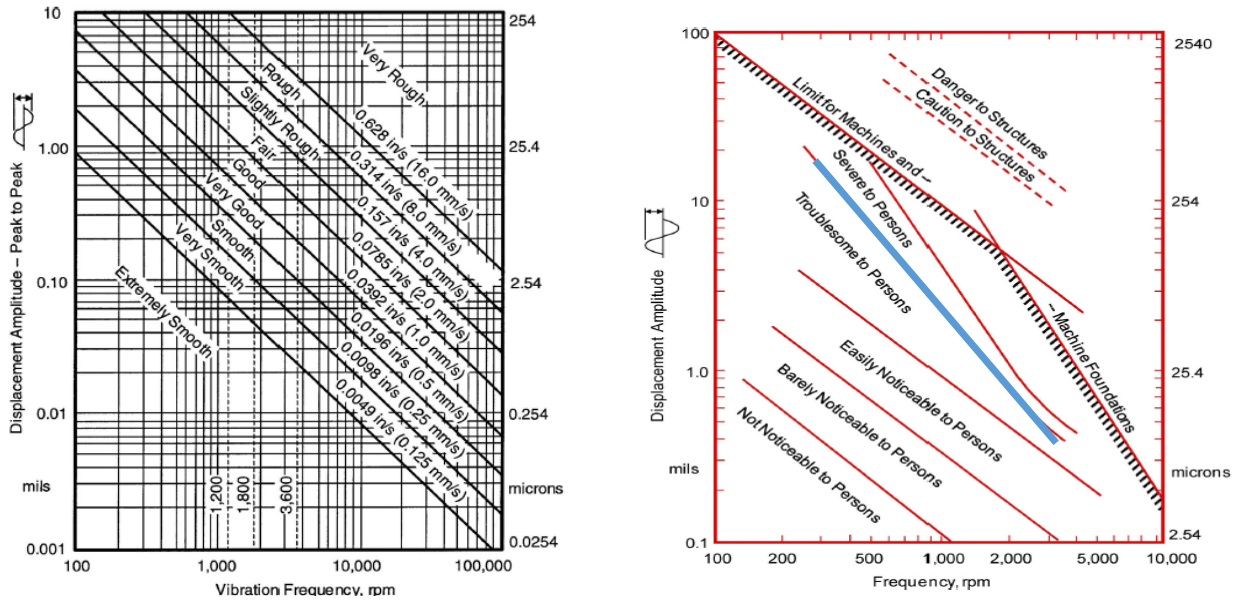

(a) (b)

Fig. 3**:** Machine vibration charts; (a) Baxter and Bernhart chart for machine performance; (b) Reiher–Meister chart for human tolerance.

where G and ρ are the shear modulus and density of the subsoil, respectively, and r is the foundation radius. The minimum frequency is 5 Hz when G, ρ, and r equal 10000 kPa, 1.51 t/m^3, and 2.5 m, respectively. The other two frequencies were set to 20 and 80 Hz to cover the frequencies used in practice.

The modified mass ratio ($B_v = \frac{1-\mu}{4}\frac{m}{\rho r^3}$) was computed to investigate the influence of the foundation mass on the liquefaction potential; where μ and m are the Poisson ratio of the subsoil and the foundation mass, respectively. Because the subsoil was saturated and the condition was undrained, a Poisson ratio of 0.45 (close to 0.5) was considered. The modified mass ratios were set to 0.001, 0.05, 0.12, and 0.23, corresponding to foundation thicknesses of 0.01, 0.1, 0.3, and 0.6 m, respectively. Notably, B_v of 0.001 indicates a massless foundation. cement content percentages (5 and 10%) were used to treat the sabkha layer. Furthermore, the thickness of the treated sabkha layer was set as 0.12, 0.24, and 0.48 times the foundation diameter.

RESULTS AND DISCUSSIONS

To examine the liquefaction of sabkha on massless or mass-vibrating foundations, the PWP ratios (r_u) at different levels in the natural sabkha profile were evaluated. (r_u) is defined as the ratio of the excess PWP at a given dynamic time to the initial effective stress (effective stress at the start of vibration loading). Figure 4 shows the effective stress history at a depth of 0.5 m under the massless foundation that rested immediately on the natural sabkha for frequency and displacement amplitude of 80 Hz and 0.04 mm, respectively. The effective stress reached zero (liquefaction) after a few cycles (6th cycle). Figure 5 shows the effect of the frequency of the vibrating foundation on r_u at different depths below the centerline of the foundation. The PWP ratio equals unity just beneath the foundation, and decreases with depth. The liquefied zone (the zone in which r_u equals unity) starts at the base of the foundation and increases with the operating frequency

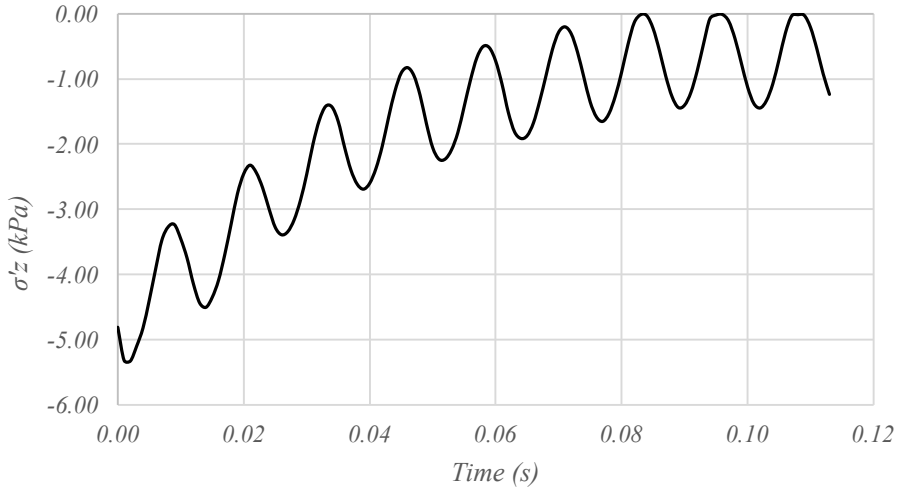

Fig. 4**:** Time history of effective stress (σ_z') at a depth 0.5 m below the vibration foundation at the operating frequency of 80 Hz.

Figure 12 shows the typical change in the PWP ratio with depth along the centerline for different B_v. The induced displacement amplitude and operating frequencies were 0.04 mm and 20 Hz, respectively. The largest increase in the PWP was observed immediately below the foundation. The PWP ratio r_u generally decreases with depth because an increase in the effective stress induced by the weight of the soil with depth decreases r_u. Beaty and Perlea (Beaty & Perlea, 2011) considered liquefied zones with a maximum r_u greater than 0.7 to be liquefied. Fig. 6 shows that, at a foundation level, B_v of 0.0028 and 0.058 corresponds to maximum r_u of 1.0 and 0.74, respectively. However, the maximum pore pressure ratio for B_v of 0.17 and 0.3 are approximately 0.43 and 0.36, respectively, which indicates a non-liquefiable condition. The foundation mass has two effects (positive and negative). The positive effect of the foundation mass was an increase in the effective stress of the sabkha soil particles and a decrease in the value of r_u by at least 0.3. However, the negative effect is that the inertial forces of the foundation increase the value of r_u; however, based on the FEM results, the inertial forces may have a minimal effect. In addition, by interpolating the value *of* B_v and the corresponding value of r_u, the mass ratio that initiates liquefaction is 0.1445 during a 5-s operation. Therefore, the minimum mass ratio required to prevent the liquefaction at a dimensionless frequency (α) of less than 9.96 is 0.1445. The dimensionless frequency depends on the angular frequency (ω), r the foundation radius (r), and the subsoil condition in terms of density (ρ) and shear modulus (G). It was represented as [$\alpha = \omega r\sqrt{(\rho \ / \ G)}$]. In other words, the minimum foundation mass that prevents liquefaction in sabkha soil depends on the ratio of machine velocity to shear wave velocity of the subsoil (sabkha).

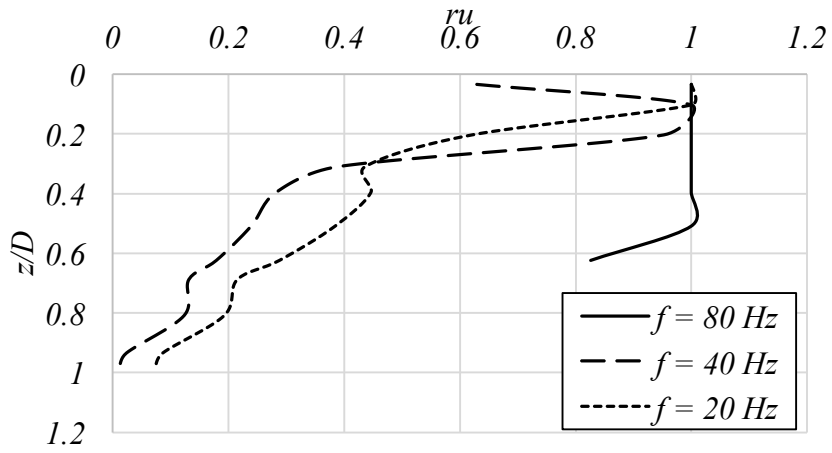

Fig. 5: PWP ratio with depth under massless vibration foundation at several frequencies at t = 5 sec, under displacement amplitude A_z = 0.04 mm.

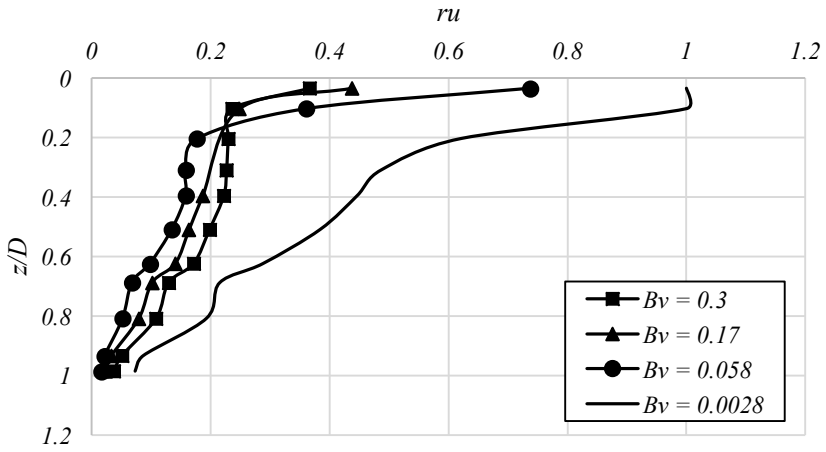

Fig. 6: Influence of foundation's mass on PWP ratio.

Numerical and experimental studies conducted by Fattah et al. (2015) and Fattah et al. (2017) on shallow foundations that rested on saturated soil and were subjected to vertical harmonic loading at different frequencies showed no liquefaction in the supported saturated sand. These results agree with those of the present study in terms of the mass foundation resting on saturated sabkha soil. To simplify the analysis, 4 assumptions were made: (1) the type of machine foundation is a block foundation; (2) the subsoil is saturated sabkha soil; (3) the embedment depth is zero; and (4) the cross-section shape of the foundation is circular with a diameter of 5 m.

CONCLUSIONS

In this study, the effect of a machine foundation under vertical vibration loading on the liquefaction potential of sabkha soil (subsoil) was investigated using numerical analysis. The parameters studied include vertical displacement amplitude (400, 40, and 4 μm), frequency (5, 20, and 80 Hz), foundation mass modified mass ratio of foundation (Bv = 0.0028, 0.058, 0.17, and 0.3). The sabkha soil was modeled using the UBC-PLM constitutive model based on the static and dynamic properties of the soil. The circular foundation was modeled as a linear elastic concrete material, and the foundation diameter was maintained constant at 5 m. Dynamic modelling issues in terms of element size, time increment, and viscous boundary conditions were considered. The pore water pressure (PWP) ratio (r_u), defined as the ratio of pore water pressure to the initial effective stress of points at different levels in the natural sabkha soil profile under a vibrating foundation, was evaluated. The main finding was that r_u increased with depth and decreased thereafter. The operating frequency of the vertical vibration loading increased PWP. For massless foundation (Bv = 0.0028, massless foundation) and foundation with a thickness of 0.15 m (Bv = 0.058), liquefaction was observed in the sabkha soil at a depth close to the subsurface, and the corresponding maximum r_u was 1.00 and 0.74, respectively. The variation in r_u in the sabkha increases with decreasing foundation mass.

Acknowledgments

The authors acknowledge the Researchers Supporting Project number (RSP2023R285), King Saud University, Riyadh, Saudi Arabia.

Funding

Researchers Supporting Project number (RSP2023R285), King Saud University, Riyadh, Saudi Arabia.

REFERENCES

Ahmed, H. R. & Al Shayea, N. A. 2017. Seismic behavior and zoning of the sabkha soils in Jubail industrial city, Saudi Arabia. *Journal of Seismology*. https://doi.org/10.1007/s10950-017-9657-1

Al-Amoudi, O. S. B. & Abduljauwad, S. N. 1994. Modified odometer for arid, saline soils. *Journal of Geotechnical Engineering*, *120*(10), 1892–1897.

Al-Amoudi, O. S. B. & Abduljauwad, S. N. 1995. Compressibility and collapse characteristics of arid saline sabkha soils. *Engineering Geology*. https://doi.org/10.1016/0013-7952(95)00016-9

Al-Shamrani, M. A. 2004. Applicability of the rectangular hyperbolic method to settlement predictions of sabkha soils. *Geotechnical and Geological Engineering*. https://doi.org/10.1023/B:GEGE.0000047046.73649.04

Al-Shamrani, M. A. & Dhowian, A. W. 1996. Characterization of secondary compression behavior of Sabkhasoils. *Engineering Geology*.

A**lnuaim, A., Alsanabani, N. & Alshenawy, A. 2020**. Monotonic and Cyclic Behavior of Salt-Encrusted Flat (Sabkha) Soil. *International Journal of Civil Engineering*, 1–12.

A**mini, F. & Qi, G. Z. 2000**. Liquefaction testing of stratified silty sands. *Journal of Geotechnical and Geoenvironmental Engineering*, *126*(3), 208–217.

ASTM D2216-10. 2010. Standard test methods for laboratory determination of water (Moisture) Content of Soil and Rock by Mass 1. *ASTM International*. https://doi.org/10.1520/D2216-10

ASTM D422. 2007. Standard test method for particle-size analysis of soils. *ASTM International*.

https://doi.org/10.1520/D0422-63R07E02

ASTM D4318-10. 2010. Standard test methods for liquid limit, plastic limit, and plasticity index of soils. *ASTM International*. https://doi.org/10.1520/D4318-10

ASTM D6938–10. 2010. Standard test method for in place density and water content of soil and soil aggregate by nuclear methods (Shallow Depth). *ASTM International*. https://doi.org/10.1520/D6938-10

ASTM D854. 2010. Standard test for specific gravity of soil solids by water pycnometer. In *ASTM International*. https://doi.org/10.1520/D0854-10

Bathe, K.-J. 2006. *Finite element procedures*. Klaus-Jurgen Bathe.

Beaty, M. H. & Perlea, V. G. 2011. Several observations on advanced analyses with liquefiable materials. *Proceedings of the 31st Annual USSD Conference and 21st Conference on Century Dam Design-Advances and Adaptations*, 1369–1397.

Bhatia, K. G. 2008. Foundations for industrial machines and earthquake effects. *ISET Journal of Earthquake Technology*, *45*(1–2), 13–29.

Budhu, M. 2015. Soil Mechanics Fundamentals. John Wiley & Sons.

El Fiky, N. E., Metwally, K. G. & Akl, A. Y. 2020. Effect of top soil liquefaction potential on the seismic response of the embedded piles. *Ain Shams Engineering Journal*, *11*(4), 923–931.

Fattah, M. Y., Al-Mosawi, M. J., & Al-Americ, A. F. I. 2017. Stresses and pore water pressure induced by machine foundation on saturated sand. *Ocean Engineering*, *146*, 268–281.

Fattah, M. Y., Salim, N. M., & Al-Shammary, W. T. 2015. Effect of embedment depth on response of machine foundation on saturated sand. *Arabian Journal for Science and Engineering*, *40*(11), 3075–3098.

Ibrahim, K. M. H. I. 2014. Liquefaction analysis of alluvial soil deposits in Bedsa southwest of Cairo. *Ain Shams Engineering Journal*, *5*(3), 647–655.

Kramer, S. L. 1996. Geotechnical earthquake engineering. Pearson Education India.

Lee, C. Y. 2007. Earthquake-induced settlements in saturated sandy soils. *ARPN Journal of Engineering and Applied Sciences*, *2*(4), 6–13.

Mokhtar, A.-S. A., Abdel-Motaal, M. A. & Wahidy, M. M. 2014. Lateral displacement and pile instability due to soil liquefaction using numerical model. *Ain Shams Engineering Journal*, *5*(4), 1019–1032.

MUÑOZ, B. O. M. **2008**. Plaxis version 8 dynamics manual.

Nikam, Sachin Kumar, and Sandeep Jaiswal. Experimental And Finite Element Analysis Of Nonaxisymmetric Stretch Flanging Process Using AA 5052. Journal Engineering Research. https://doi.org/10.36909/jer.ICIPPSD.15501

Petalas, A. & Galavi, V. 2013. Plaxis liquefaction model ubc3d-plm. *Plaxis Report*.

Rollins, K. M. & Seed, H. B. 1990. Influence of buildings on potential liquefaction damage. *Journal of Geotechnical Engineering*, *116*(2), 165–185.

Seed, H. B., Idriss, I. M., & Arango, I. 1983. Evaluation of liquefaction potential using field performance data. *Journal of Geotechnical Engineering*, *109*(3), 458–482.

Srivastava, Shubham, and Rajesh Kumar. Analyse the effect of Soil-Structure Interaction on Seismic Response of Building Cluster by Variation in Soil and Building Properties. Journal of Engineering Research 10 (2022)

Vaid, Y. P. & Thomas, J. 1995. Liquefaction and postliquefaction behavior of sand. *Journal of Geotechnical Engineering*, *121*(2), 163–173.

Yoshimi, Y. 1967. An experimental study of liquefaction of saturated sands. *Soils and Foundations*, *7*(2), 20–32.

Zeghal, M. & Elgamal, A.-W. **1994**. Analysis of site liquefaction using earthquake records. *Journal of Geotechnical Engineering*, *120*(6), 996–1017.